DOI: 10.18721/JPM.12404
УДК 538.915+975; 544.22.022.343; 544.225.22+25

ELASTIC CONDUCTIVITY OF SILICENE AND GERMANENE NANORIBBONS

O.S. Lebedeva[1,2], *N.G. Lebedev*[1], *I.A. Lyapkosova*[2]

[1] Volgograd State University, Volgograd, Russian Federation;

[2] Volgograd State Agricultural University, Volgograd, Russian Federation

The theoretical research results for piezoresistive properties of ideal silicene and germanene nanoribbons with different conductivity types have been presented. Within the framework of the Hubbard model, the band structure of the nanoparticles under investigation was simulated and a longitudinal component of their elastoconductivity tensor was analytically calculated. For this tensor, the dependences on the relative strain of longitudinal compression/tension as well on the nanoribbon width were studied.

Keywords: 2D structure, silicene, germanene, stress-strain state, piezoresistive effect, elastroconductivity tensor

Citation: Lebedeva O.S., Elastic conductivity of silicene and germanene nanoribbons, St. Petersburg Polytechnical State University Journal. Physics and Mathematics. 12 (4) (2019) 37–47. DOI: 10.18721/JPM.12404

ЭЛАСТОПРОВОДИМОСТЬ СИЛИЦЕНОВЫХ И ГЕРМАНЕНОВЫХ НАНОЛЕНТ

О.С. Лебедева[1,2], *Н.Г. Лебедев*[1], *И.А. Ляпкосова*[2]

[1] Волгоградский государственный университет, г. Волгоград, Российская Федерация;

[2] Волгоградский государственный аграрный университет,

г. Волгоград, Российская Федерация

Представлены результаты теоретического исследования пьезорезистивных свойств идеальных силиценовых и германеновых нанолент с разным типом проводимости. В рамках модели Хаббарда проведено моделирование зонной структуры исследуемых наночастиц и аналитический расчет продольной компоненты тензора эластопроводимости, а также исследованы его зависимости от величины относительной деформации продольного сжатия (растяжения) и ширины наноленты.

Ключевые слова: двумерная структура, силицен, германен, напряженно-деформированное состояние, пьезорезистивный эффект

Ссылка при цитировании: Лебедева О.С. Эластопроводимость силиценовых и германеновых нанолент // Научно-технические ведомости СПбГПУ. Физико-математические науки. 2019. Т. 12. № 4. С. 38–49. DOI: 10.18721/JPM.12404

Introduction

New carbon-based nanostructures synthesized in 2004, such as graphene and graphene nanoribbons, proved to be materials with a unique set of physicochemical properties that can be used in a wide range of applied problems [1–4]. The electronic characteristics of graphene vary and depend on the nature and concentration of structural defects, atoms and atomic groups adsorbed on its surface. Graphene is one of the main candidates for components of future nanoelectronics, instead of silicon. The main obstacle to widespread use of graphene in electronics is its band structure, characterized by narrow band gap; there is ongoing research focused on expanding it.

Silicene, a material similar to graphene, consisting of a two-dimensional layer of silicon atoms that make up two sublattices displaced relative to each other, was theoretically predicted in 1994 and synthesized for the first time in 2010 [5]. The width of the band gap can be controlled using an electric field, making it possible to construct an effective spin polarizer. This material attracts considerable attention due to its diverse potential applications in silicon electronics and spintronics.

Another material similar to graphene was synthesized in 2014: germanene, which, like silicene, has two atomic sublattices displaced relative to each other. The narrow band gap of germanene can be controlled by electric field, adsorption of different atoms, deformation, and interaction with the substrate [6, 7]. Germanene has great potential for applications in solar cells [8]. The calculated Grüneisen parameter of the new material indicates that the dependence on strain is similar to that for silicene [9].

Density functional theory was used in [10] to conduct a comparative study on the mechanical properties of single-layer silicene, germanene, and stanene. It was found that applying a uniaxial load to each material can alter the electronic nature of buckled structure of the semiconductor to metallic character.

Optical properties of silicene and germanene under uniform compression strain were investigated within density functional theory in [11]. The results indicate that the response of the optical field strongly depends on the magnitude of the applied load. With compression strain applied in silicene and germanene, the band gap decreases at the Dirac points and ultimately reaches zero. Absorption of light along the zigzag direction is greater than in the armchair direction in both structures.

A new direction of condensed matter physics that has evolved in recent years is straintronics. It uses physical phenomena in matter induced by deformations arising in micro-, nano- and heterostructures with external controlling fields, altering the electronic structure of this matter, and, as a result, modifying its electrical, magnetic, optical and other properties [12].

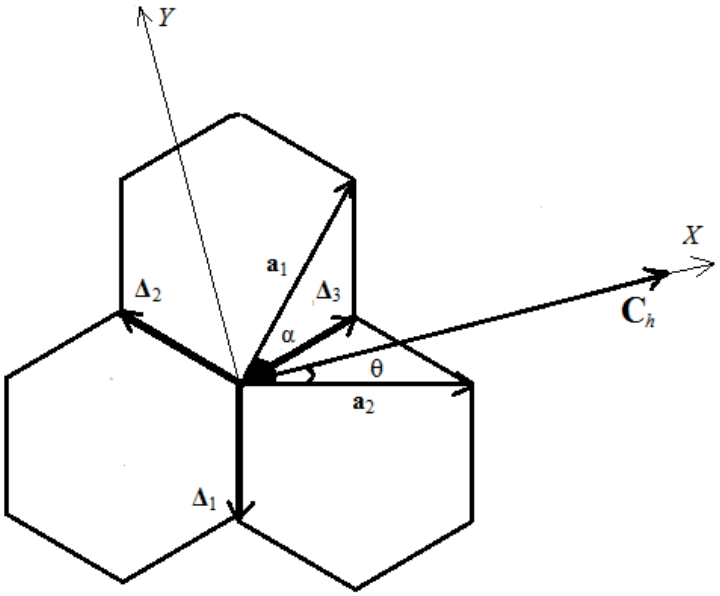

Fig. 1. Fragment of nanoribbon structure with selected coordinate system:
Δ_1, Δ_2, Δ_3 are the vectors of distance between the nearest neighbors; $\mathbf{a}_1$, $\mathbf{a}_2$ are the translation vectors; α is the angle between the translation vectors; θ is the chiral angle; $\mathbf{C}_h$ is the chiral vector

Such effects make it possible to create a new generation of information-sensing devices. For example, a transistor based on graphene with strain-induced suppression of ballistic conductivity (piezoconductivity) was proposed in [13]. Similar transistors can also be developed based on germanene and silicene; effects of strain in these materials are the focus of much research.

This paper presents the results of theoretical study on the piezoresistive properties of perfect silicene (Si) and germanene (Ge) nanoribbons (NR), SiNR and GeNR.

Model of electronic structure of deformed graphene nanoribbons

A two-dimensional hexagonal graphene layer was chosen as a geometric model of the nanoribbon. Fig. 1 shows a fragment of such a crystalline structure, with the chiral vector

$$\mathbf{C}_h = n\mathbf{a}_1 + m\mathbf{a}_2,$$

the angle α between the primitive translation vectors $\mathbf{a}_1$ and $\mathbf{a}_2$, as well as the interatomic distance vectors Δ_i.

The coordinate system is selected so that the ribbon width is measured along the *OX* axis using the chiral vector $\mathbf{C}_h$, and the *OY* axis is directed along the length of the ribbon. The angle θ between the vectors $\mathbf{C}_h$ and $\mathbf{a}_1$, counted from the translation vector $\mathbf{a}_1$, lies in the range from 0° to 30° and is called the chiral angle [4].

A mathematical model of the electronic structure of undeformed nanoribbons is constructed based on their geometric structure and the band structure of the hexagonal layer. The band structure of nanoribbons within the framework of the strong coupling method using Hückel approximations and approximate nearest neighbors has the following general form [4]:

$$\begin{aligned}\varepsilon(\mathbf{k}) &= \pm\gamma_0\left\{3+2\cos\left(\mathbf{k}\mathbf{a}_1\right)+\right.\\ &\left.+2\cos\left(\mathbf{k}\mathbf{a}_2\right)+2\cos\left(\mathbf{k}\left(\mathbf{a}_1-\mathbf{a}_2\right)\right)\right\}^{1/2} =\\ &= \pm\gamma_0\\ &\left\{1+4\cos\left(\frac{\mathbf{k}\left(\mathbf{a}_1+\mathbf{a}_2\right)}{2}\right)\cos\left(\frac{\mathbf{k}\left(\mathbf{a}_1-\mathbf{a}_2\right)}{2}\right)\right.\\ &\left.+4\cos^2\left(\frac{\mathbf{k}\left(\mathbf{a}_1-\mathbf{a}_2\right)}{2}\right)\right\}^{1/2},\end{aligned} \tag{1}$$

where γ_0 is the hopping integral, the matrix element of electron transition between neighboring atoms; **k** is the wave vector, one of the components of which is quantized along the width of the ribbon.

The Fermi level in dispersion relation (1) is taken as 0 eV.

The condition for quantization of the wave vector **k** along the direction of the chiral vector $\mathbf{C}_h$ can be written as follows [4]:

$$\mathbf{k}\cdot\mathbf{C}_h = 2\pi q,\ q = 1, 2, \ldots . \tag{2}$$

The components of the wave vector k_x and k_y should be chosen so that they are codirectional with the chiral vector $\mathbf{C}_h$ and the length of the nanoribbon, respectively, i.e.,

$$\mathbf{k}_x \uparrow\uparrow \mathbf{C}_h,\ \mathbf{k}_y \perp \mathbf{C}_h.$$

The magnitude of the chiral vector of undeformed nanoribbons can be represented, in accordance with its definition, in the following known form [1]:

$$\begin{aligned}\left|\mathbf{C}_{\mathbf{h}0}\right| &= \sqrt{n\cdot\mathbf{a}_1^2 + m\cdot\mathbf{a}_2^2 + 2nm\mathbf{a}_1\mathbf{a}_2} =\\ &= a\sqrt{n^2+m^2+nm}.\end{aligned} \tag{3}$$

Using representation (3) and conditions (2), we can obtain an explicit expression for quantization of the transverse component of the wave vector:

$$\begin{aligned}k_x a &= \frac{2\pi q}{\sqrt{n^2+m^2+nm}},\\ q &= 1,2,\ldots,\left[\sqrt{n^2+m^2+nm}\right].\end{aligned} \tag{4}$$

Arguments of trigonometric functions in expression (1) for band structure can be written, based on geometric transformations corresponding to Fig. 1, as follows:

$$\begin{aligned}\frac{\mathbf{k}(\mathbf{a}_1+\mathbf{a}_2)}{2} &= \left(\frac{1}{\sqrt{n^2+m^2+nm}}\times\right.\\ &\left.\times\left(\frac{3\pi q(n+m)}{2\sqrt{n^2+m^2+nm}}+\frac{\sqrt{3}k_y a(n-m)}{4}\right)\right),\\ \frac{\mathbf{k}(\mathbf{a}_1-\mathbf{a}_2)}{2} &= \left(\frac{1}{\sqrt{n^2+m^2+nm}}\times\right.\\ &\left.\times\left(\frac{\pi q(n-m)}{2\sqrt{n^2+m^2+nm}}-\frac{\sqrt{3}k_y a(n+m)}{4}\right)\right).\end{aligned} \tag{5}$$

As a result, expression (1) and relations (5) completely determine the energy spectrum of electrons of undeformed nanoribbons.

According to theory of electronic structure of graphene nanoribbons [4], a set of dispersion curves of the electronic spectrum, numbered by the integer q, is formed by crossing the two-dimensional energy surface of graphene with parallel planes corresponding to the continuous component of the wave vector. The position of these planes relative to the Brillouin zone is determined by the value of the discrete k_x component of the wave vector (in accordance with quantization condition (2)).

The deformed state of a crystallite is generally characterized by a distortion tensor,

$$u_{\mu\eta} = \partial_\eta \left(\mathbf{r}' - \mathbf{r}\right)_\mu, \left(\mu, \eta = x, y, z\right),$$

where **r, r'** are the radius vectors of the initial and final position of some point of the crystallite [14].

The diagonal elements of the tensor characterize the relative elongation of the sample along the corresponding direction, the off-diagonal elements determine the rotation angle of the linear element under strain.

In accordance with the definition of the distortion tensor, the energy spectrum of deformed nanoribbons is formulated by modifying the scalar products that appear in the arguments of trigonometric functions in expression (1) for the electronic spectrum. The change in the primitive cell of a nanoribbon under tensile load is shown in Fig. 2. The figure illustrates the model where strain induces not only the change in interatomic bond lengths, Δ_i ($\Delta_i = R_0(1 + \delta)$), by their relative elongation δ ($\delta = \Delta R/R_0$) but also in the angle α between the translation vectors ($\alpha = \alpha_0 + \Delta\alpha$, where $\alpha_0 = \pi/3$ is the angle between the translation vectors in the undeformed lattice, $\Delta\alpha$ is the angle change due to deformation), and, therefore, in the projections of the translation vectors $\mathbf{a}_1$ and $\mathbf{a}_2$ on the OX and OY axes of the selected coordinate system.

The expression for the band structure of deformed nanoribbons can be obtained based on geometric transformations (see Fig. 2). As a result, the electronic spectrum of such nanoribbons within the framework of the strong binding method takes the form

$$\varepsilon(\mathbf{k}) = \pm\gamma\left(1 + 4\cos\left[\pi n A_1 + B_1\right]\times\right.$$
$$\times\cos\left[\pi n A_2 - B_2\right] +$$
$$\left. +4\cos^2\left[\pi n A_2 - B_2\right]\right)^{1/2}, \quad (6)$$

where the following notations are introduced for the general case:

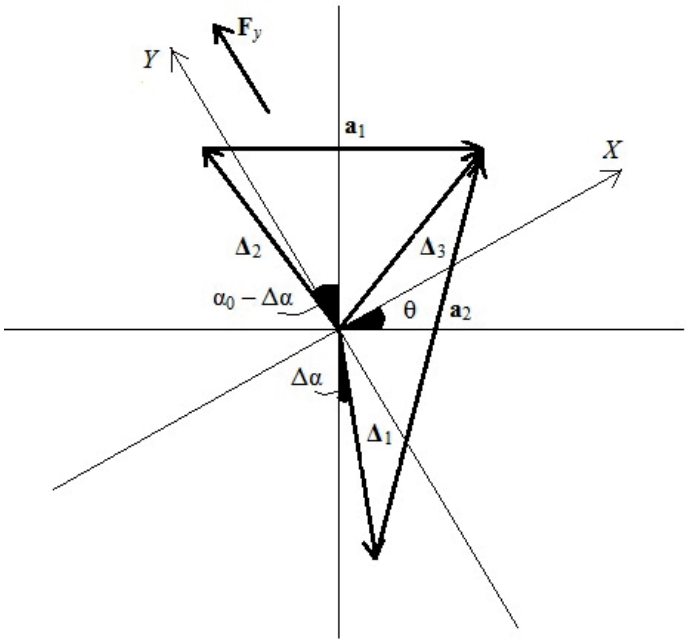

Fig. 2. Positions of interatomic vectors Δ_1, Δ_2, Δ_3 after tensile or compressive strain taking into account their rotation through the angle $\Delta\alpha$; $\mathbf{F}_y$ is the tensile (compressive) force. The remaining notations are given in the caption to Fig. 1

$$A_1 = \frac{F\cos\alpha + G\sin\alpha}{A\cos\alpha + B\sin\alpha},$$
$$B_1 = k_y R_0(1+\delta)\left(-G\cos\alpha + F\sin\alpha\right),$$
$$A_2 = \frac{-E\cos\alpha}{A\cos\alpha + B\sin\alpha},$$
$$B_2 = k_y R_0(1+\delta)E\sin\alpha,$$
$$A = n\sin\theta\cos(2\alpha_0) + m\cos\theta\cos\left(\alpha_0/2\right), \quad (7)$$
$$B = \sin\theta\left[n\sin(2\alpha_0) + m\cos\left(\alpha_0/2\right)\right],$$
$$E = \sin\theta\sin\left(\alpha_0/2\right) + \cos\theta\cos\left(\alpha_0/2\right),$$
$$F = \sin\theta\cos(2\alpha_0) + \cos\theta\cos\left(\alpha_0/2\right),$$
$$G = \sin\theta\left[\sin(2\alpha_0) + \cos\left(\alpha_0/2\right)\right].$$

The change in the transverse dimensions (width) of the nanoribbon due to strain is taken into account by modifying the magnitude of the chiral vector $\mathbf{C}_h$, which, in accordance with the definition of Poisson's ratio and direct proportionality of the main geometric dimensions of nanotubes to the lattice parameters, can be calculated by the following formula:

$$C_h = (1 - \boldsymbol{\nu}\cdot\boldsymbol{\delta})\, C_{h0}, \quad (8)$$

where ν is Poisson's ratio whose value varies in the range $\nu = 0.19$–0.27.

Relation (8) and the selected geometric model of deformed nanoribbons make it possible to find the angle α between the translation vectors in the deformed hexagonal lattice included in the expressions for coefficients (7) of the nanoribbon spectrum (6):

$$\sin\alpha = \frac{BC + A\sqrt{B^2 - C^2 + A^2}}{A^2 + B^2}, \quad (9)$$

where

$$C = \frac{1-\nu\delta}{1+\delta}\left[\sin\theta\left(n\cos\alpha_0 + m\cos^2\left(\alpha_0/2\right)\right) + \right.$$
$$\left. + \frac{m}{2}\cos\theta\sin\alpha_0\right],$$

and the coefficients A and B are expressed by Eq. (8).

The procedure for calculating the dependence of the hopping integral γ on the relative strain δ using carbon nanotubes as an example is described in detail in [15–18].

The following values of relative tensile (compressivee) strain were used for theoretical calculations:

$$\delta = +0.250\ ; \pm 0.104\ ; 0.069\pm\ ; 0.035\pm.$$

Finding the band structure of perfect nanoparticles taking into account scattering effects, for example, the Coulomb interaction of electrons at one site, consists in finding the poles of Green's functions [19] within the Hubbard model [20], which is described in [17] for the case of achiral carbon nanotubes.

The electronic spectrum of the deformed nanoribbon can then be represented as

$$E(\mathbf{k}) = \frac{1}{2}\left[\varepsilon(\mathbf{k}) + U \pm \right.$$
$$\left. \pm\left(\varepsilon(\mathbf{k})^2 - 2\varepsilon(\mathbf{k})U(1-2n_{-\beta}) + U^2\right)^{1/2}\right], \quad (10)$$

where $\varepsilon(\mathbf{k})$ is the band structure of deformed perfect nanoribbons, expressed by Eq. (6); U is the energy of the Coulomb interaction of electrons at one site, which can be estimated, for example, using the semi-empirical MNDO method from quantum chemistry [21]; $n_{-\beta}$ is the number of electrons with opposite spin already located in the zone.

No fundamental qualitative differences could be found for the obtained band structures of semiconductor SiNR and GeNR nanoribbons of the armchair type, in comparison with the energy spectrum of undeformed nanowires. Quantitative analysis points to narrowing band gap, conduction and valence bands, leading to increased density of electronic states in case of compression and, conversely, broadening of these bands (decreased density of states) under tensile strain. A similar result was observed for deformed achiral (armchair and zigzag) nanotubes, as well as for achiral carbon nanotubes studied in [15–18].

Axial tension (compression) also changes the band structure of conducting armchair and zigzag SiNR and GeNR nanoribbons in the manner described above; this does not make them fundamentally different from armchair nanoribbons, except for one notable aspect: the band gap is absent in such nanoribbons and does not appear under small strain. Strain-induced opening of the band gap is observed in mixed nanoribbons, as in the case of chiral carbon nanotubes [23], where Mott-type conductor → semiconductor and semiconductor → conductor transitions due to axial tensile (compressive) strain become possible.

Elastoconductivity of nanoribbons

Simulation of piezoresistive constants, in particular, the axial component of the elastoconductivity tensor of nanowires, was carried by the technique described in detail in [15–17]. In accordance with the definition of the elastic conductivity tensor [22], its longitudinal component for quasi-one-dimensional structures can be expressed by the following formula:

$$M = \frac{\Delta\sigma}{\sigma_0}\frac{1}{\delta}, \qquad (11)$$

where M is the longitudinal component of 4th-order elastoconductivity tensor ($M = m_{zzzz}$); σ_0 is the longitudinal component of 2nd-order tensor of specific conductivity σ_{zz} of an undeformed crystal; $\Delta\sigma$ is the change in the longitudinal component of the conductivity tensor due to crystallite strain ($\Delta\sigma = \sigma - \sigma_0$, σ is the longitudinal component of the 2nd-order tensor of specific conductivity σ_{zz} of the deformed crystal).

The longitudinal component of the zero-phonon conductivity tensor of nanoribbons was calculated within the Kubo–Greenwood theory [19] using Green's function method with the Hubbard model Hamiltonian [20]. The final expression for the longitudinal conductivity of nanoribbons used in the calculations of the constant Mhas the following form [17]:

$$\sigma = 2\frac{i\pi e^2}{k_B TV}\sum_{\mathbf{k},\beta}\sum_{\mathbf{q},\lambda} v(\mathbf{k})v(\mathbf{q}) < \\ < n_{\mathbf{k}\beta} > \left[< n_{\mathbf{q}\lambda} > + \delta_{\mathbf{kq}}\delta_{\beta\lambda}\left(1 - < n_{\mathbf{k}\beta} >\right)\right], \qquad (12)$$

where V is the crystallite volume; k_B is the Boltzmann constant; T is absolute temperature; e is the elementary charge; $\mathbf{k}$, $\mathbf{q}$ are two-component wave vectors within the Brillouin zone; β, λ are the spin indices; $< n_{\mathbf{k}\beta} >$ is the average number of particles in a quantum state with the wave vector $\mathbf{k}$ and spin β, expressed by the Fermi–Dirac distribution function; v is the longitudinal component of the electron velocity vector in the Brillouin zone.

The velocity vector is found by conventional means using the electronic spectrum (10):

$$\mathbf{v}(\mathbf{k}) = \frac{1}{\hbar}\frac{\partial E(\mathbf{k})}{\partial \mathbf{k}}. \qquad (13)$$

Since numerous studies of the transport properties of Dirac materials, for example, graphene nanoribbons, point to ballistic (zero-phonon) nature of electronic conductivity [4], using the Hubbard model, which does not include the electron-phonon interaction, seems appropriate.

Figs. 3 and 4 show the component M of the elastic conductivity tensor depending on the relative strain δ equal to

$$-0.067,\ -0.045,\ -0.022,\\ +0.022,\ +0{,}045,\ +0.067,\ +0.250$$

for armchair (Arm) and zigzag (Zg) SiNR and GeNR nanoribbons of different widths: nArm (n = 9, 10, 50 and 100) and mZg (m = 5 and 10) (the values are given in primitive cells). Numerical results were obtained at T = 300 K. The calculated points are connected by solid lines to visually illustrate the trend in the variation of the constant M. Notably, the point $\delta = 0$ is not defined.

As follows from Figs. 3 and 4, the longitudinal component M of conducting armchair (9Arm) and zigzag (5Zg, 10Zg) nanoribbons is positive, and the behavior of this component completely correlates with the changes in the band structure of the nanoribbons, described above. A common trend for the given conducting nanoribbons is monotonic growth (or decrease) of M with increasing relative tensile (compressive) strain δ. A similar behavior is observed for conducting achiral carbon nanotubes [16, 17]. Despite the increase in the width of the conduction band and the decrease in the density of states at the Fermi level with increasing δ, the specific conductivity of the objects increases, which leads to monotonic growth of the component M. The reason for this effect is that the increasing number of charge carriers with increasing energies contribute to specific conductivity of the crystallite. Thermal fluctuations lead to filling of the conduction band of the nanoribbon by electrons according to the Fermi–Dirac distribution function. Modification of the electronic spectrum leads to a change in specific conductivity, taking into account all possible filled electronic states, and, consequently, to increase in the component M with increasing δ.

The longitudinal component M is negative for semiconductor armchair (10Arm, 50Arm, 100Arm) SiNR and GeNR nanoribbons but also monotonically

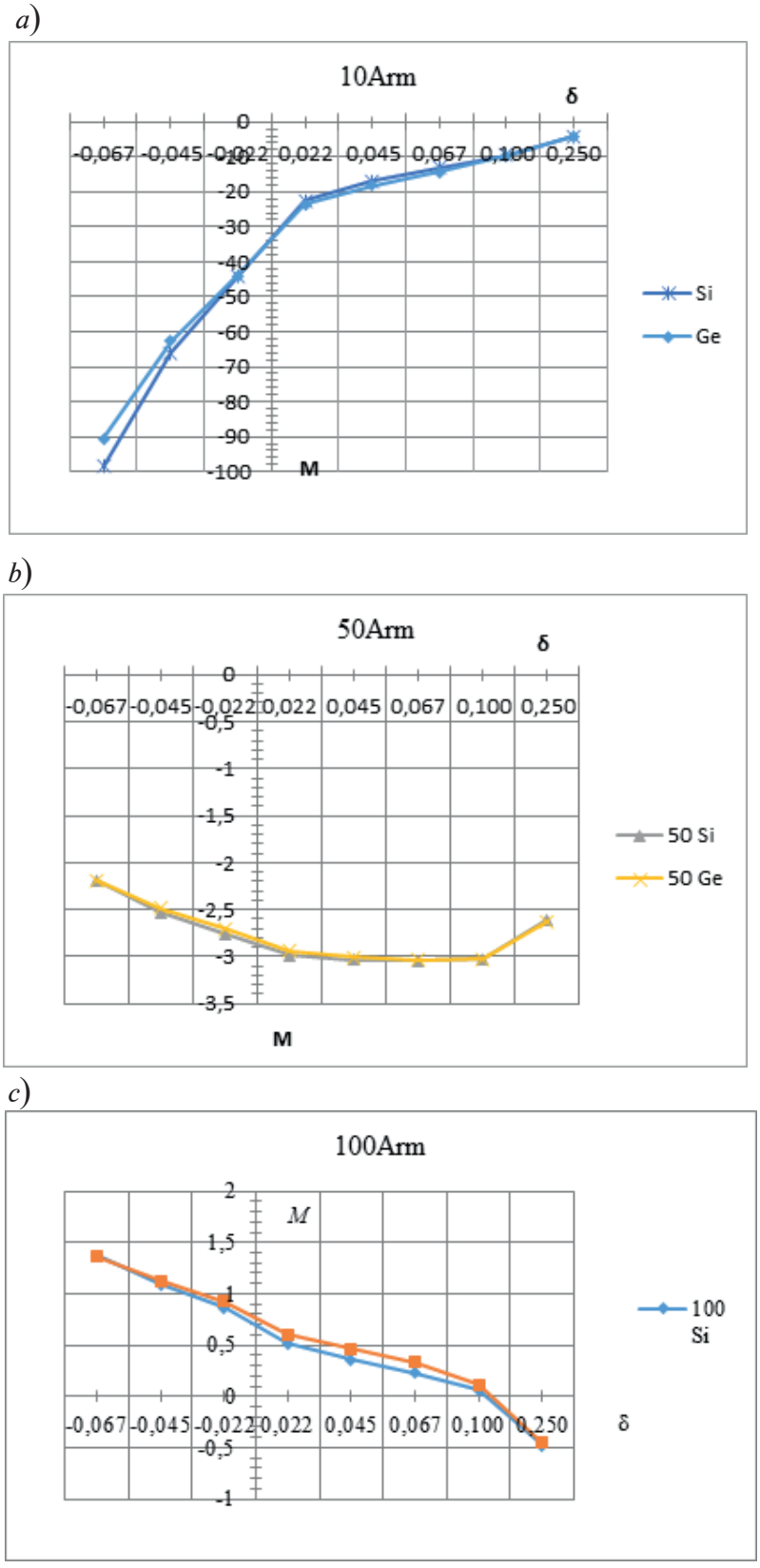

Fig. 3. Longitudinal component M of elastic conductivity tensor of armchair (Arm) SiNR and GeNR nanoribbons with a width of 10 (*a*), 50 (*b*) and 100 (*c*) primitive cells as function of relative strain δ. The point $\delta = 0$ is not defined on all curves.

increases with increasing δ, the same as in case of conducting nanoribbons. The negative value is due to a decrease in conductivity with increasing strain. This effect is also a consequence of the behavior of the band structure of deformed semiconductor nanoribbons, where the band gap broadens and, therefore, the number of occupied states in the conduction band decreases. A similar behavior of the constant M is observed for conducting achiral carbon nanotubes [16, 17].

Applying the above-described technique for calculating the longitudinal component of the elastic conductivity tensor to study of piezoresistive properties of carbon nanotubes [16, 17] yielded results that are in good agreement with the data given in literature on the piezoresistive properties of carbon structures [24, 25]. Therefore, it should be expected that due to similar approaches to describing the band structure, graphene nanoribbons (Dirac structures) possess qualitatively identical piezoresistive properties. There are as yet no data in literature relating to nanoribbons of the graphene family, including silicene and germanene.

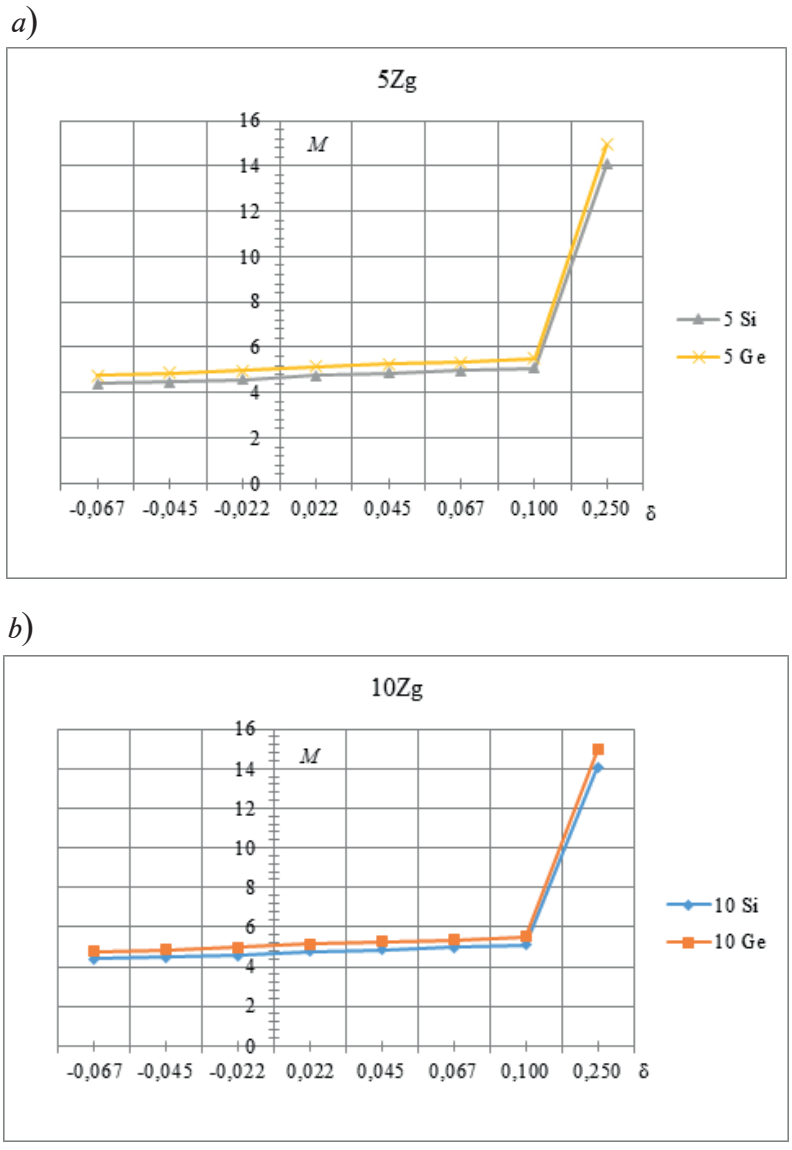

Fig. 4. Longitudinal component M of elastic conductivity tensor of zigzag (Zg) SiNR and GeNR nanoribbons with a width of 5 (*a*) and 10 (*b*) primitive cells as function of relative strain δ.
The point δ = 0 is not defined on all curves.

Conclusion

We have carried out theoretical study of piezoresistive properties of perfect silicene and germanene nanoribbons with different types of conductivity within the framework of the Hubbard model, finding several peculiarities in the behavior of the longitudinal component of the elastoconductivity tensor, described above. Quantitative study of the constant M depending on the magnitude of the strain and the width of the nanoribbon yields a more complete picture of the variation in the conductivity of nanoribbons due to tensile or compressive strain. In addition, the longitudinal component of the elastic conductivity tensor of germanene nanoribbons slightly exceeds the component of silicene nanoribbons.

The results obtained can be used for developing electromechanical nanosensors based on the piezoresistive effect, whose main structural element are silicene and germanene nanoribbons.

The study was financially supported by the Russian Foundation for Basic Research as part of scientific project no. 18-31-00130.

REFERENCES

1. **Morozov S.V., Novoselov K.S., Geim A.K.,** Electronic transport in graphene, Phys. Usp. 51 (7) (2008) 744–748.

2. **Lozovik Yu.E., Merkulova S.P., Sokolik A.A.,** Collective electron phenomena in graphene, Phys. Usp. 51 (7) (2008) 727–744.

3. **Chernozatonskii L.A., Sorokin P.B., Artukh A.A.**, New nanostructures based on graphene: physical and chemical properties and applications, Russ. Chem. Rev. 83 (2014) 251–279.

4. Physics of graphene, Edited by Aoki H., Dresselhaus M.S. (Nanoscience and Technology), Springer International Publishing, 2014.

5. **Gert A.V., Nestoklon M.O., Yassievich I.N.,** Band structure of silicene in the tight binding approximation, JETP. 121 (1) (2015) 115–121.

6. **Acun A., Zhang L., Bampoulis P., et al.,** Germanene: the germanium analogue of graphene, Journal of Physics: Condensed Matter. 27 (44) (2015) 443002.

7. **Behzad S.,** Effect of uni-axial and bi-axial strains and vertical electric field on free standing buckled germanene, Journal of Electron Spectroscopy and Related Phenomena. 229 (December) (2018) 13–19.

8. **Ould NE M.L., El hachimi A.G., Boujnah M., et al.,** Comparative study of electronic and optical properties of graphene and germanene: DFT study, Optik. 158 (April) (2018) 693–698.

9. **Kaloni T.P., Schwingenschlugl U.**, Stability of germanene under tensile strain, Chemical Physics Letters. 583 (17 September) (2013) 137–140.

10. **Mortazavi B., Rahaman O., Makaremi M., et al.,** First-principles investigation of mechanical properties of silicene, germanene and stanine, Physica E: Low-dimensional Systems and Nanostructures. 87 (March) (2017) 228–232.

11. **Kazemlou V., Phirouznia A.,** Influence of compression strains on photon absorption of silicene and germanene, Superlattices and Microstructures. 128 (April) (2019) 23–29.

12. **Bukharaev A.A., Zvezdin A.K., Pyatakov A.P., Fetisov Yu.K.,** Straintronics: a new trend in micro- and nanoelectronics and material science, Phys. Usp. 61 (12) (2018) 1175–1212.

13. **McRae A.C., Wei G., Champagne A.R.**, Graphene quantum strain transistors, Physical Review Applied. 11 (5) (2019) 054019.

14. **Landau L.D., Lifshitz E.M.,** Theory of elasticity, 2nd ed., Course of theoretical physics, Vol. 7, Pergamon Press, Oxford, 1981.

15. **Lyapkosova O.S., Lebedev N.G.**, Piezoresistive effect in single-walled carbon nanotubes, Physics of the Solid State. 54 (7) (2012) 1501–1506.

16. **Lebedeva O.S., Lebedev N.G.**, The influence of the stretching and compression deformations on the piezoresistance of the carbon nanotubes and graphene nanoribbons, St. Petersburg State Polytechnical University Journal. Physics and Mathematics. (1(189)) (2014) 26–34.

17. **Lebedeva O.S., Lebedev N.G.**, The piezoresistive effect in doped single-walled carbon nanotubes in the "Hubbard-I" approach, St. Petersburg State Polytechnical University Journal. (2(195)) (2014) 149–161.

18. **Lebedeva O.S., Lebedev N.G.,** Deformation change of the band gap of impurity carbon nanotubes, Russian Journal of Physical Chemistry B: Focus on Physics. 8 (5) (2014) 745–751.

19. **Kvasnikov I.A.,** Termodinamika i statisticheskaja fizika. T. 4: Kvantovaja statistika [Thermodynamics and statistical physics, Vol. 4: Quantum Statistics], KomKniga Publ., Moscow, 2005.

20. **Izyumov Ju.A., Chashhin N.I., Alekseev D.S.,** Teorija sil'no korrelirovannyh sistem. Metod proizvodjashhego funkcionala [The theory of strongly correlated systems. Method of generating functional], Reguljarnaja i Haoticheskaja

Dinamika Publ., Moscow, 2006.

21. **Stepanov N.F.**, Kvantovaya mehanika i kvantovaya himiya [Quantum Mechanics and Quantum Chemistry]. Mir, Moscow, 2001.

22. **Bir G.L., Pikus G.E.**, Symmetry and strain-induced effects in semiconductors, John Wiley & Sons, Inc., New-York, 1974.

23. **Lebedeva O.S., Lebedev N.G., Lyapkosova I.A.**, Piezoconductivity of chiral carbon nanotubes in the framework of the tight-binding method, Mathematical Physics and Computer Simulation. 21 (1) (2018) 53–63.

24. **Li Y., Wang W., Liano K., et. al.,** Piezoresistive effect in carbon nanotube films, Chinese Science Bulletin. 48(2) (2003) 125–127.

25. **Obitayo W., Liu T.,** A review: carbon nanotube-based piezoresistive strain sensors, Journal of Sensors. 2012 (2012), ID 652438, DOI 10.1155/2012/652438.

Received 01.10.2019, accepted 09.12.2019.

THE AUTHORS

LEBEDEVA Olga S.
Volgograd State University
Volgograd State Agricultural University
100, University Ave., Volgograd, 400062, Russian Federation
26, University Ave., Volgograd, 400002, Russian Federation
lebedeva_os@volsu.ru

LEBEDEV Nikolay G.
Volgograd State University
100, University Ave., Volgograd, 400062, Russian Federation
nikolay.lebedev@volsu.ru

LYAPKOSOVA Irina A
Volgograd State Agricultural University
26, University Ave., Volgograd, 400002, Russian Federation
lyapkosova_irina@mail.ru

СПИСОК ЛИТЕРАТУРЫ

1. Морозов С.В., Новоселов К.С., Гейм А.К. Электронный транспорт в графене // Успехи физических наук. 2008. Т. 178. № 7. С. 776–780.

2. Лозовик Ю.Е., Меркулова С.П., Соколик А.А. Коллективные электронные явления в графене // Успехи физических наук. 2008. Т. 178. № 7. С. 758–776.

3. Чернозатонский Л.А., Сорокин П.Б., Артюх А.А. Новые наноструктуры на основе графена: физико-химические свойства и приложения // Успехи химии. 2014. Т. 83. Вып. 3. С. 251–279.

4. Physics of graphene. Edited by Aoki H., Dresselhaus M.S. (Nanoscience and Technology). Switzerland: Springer International Publishing, 2014. 345 p.

5. Герт А.В., Нестоклон М.О., Яссиевич И.Н. Зонная структура силицена в приближении сильной связи // Журнал экспериментальной и теоретической физики. 2015. Т. 148. № 1. С. 133–139.

6. **Acun A., Zhang L., Bampoulis P., et al.,** Germanene: the germanium analogue of graphene // Journal of Physics: Condensed Matter. 2015. Vol. 27. No. 44. P. 443002.

7. **Behzad S.** Effect of uni-axial and bi-axial strains and vertical electric field on free standing buckled germanene // Journal of Electron Spectroscopy and Related Phenomena. 2018. Vol. 229. December. Pp. 13–19.

8. **Ould N.E. M.L., El hachimi A.G., Boujnah M., Benyoussef A., El Kenz A.** Comparative study of electronic and optical properties of graphene and germanene: DFT study // Optik. 2018. Vol. 158. April. Pp. 693–698.

9. **Kaloni T.P., Schwingenschlugl U.** Stability of germanene under tensile strain // Chemical Physics Letters. 2013. Vol. 583. 17 September. Pp. 137–140.

10. **Mortazavi B., Rahaman O., Makaremi M., Dianat A., Cunibertic G., Rabczuk T.** First-principles investigation of mechanical properties of silicene, germanene and stanene // Physica E:

Low-dimensional Systems and Nanostructures. 2017. Vol. 87. March. Pp. 228–232.

11. **Kazemlou V., Phirouznia A.** Influence of compression strains on photon absorption of silicene and germanene // Superlattices and Microstructures. 2019. Vol. 128. April. Pp. 23–29.

12. Бухараев А.А., Звездин А.К., Пяток А.П., Фетисов Ю.К. Стрейнтроника – новое направление микро- и наноэлектроники и науки о материалах // Успехи физических наук. 2018. Т. 188. № 12. С. 1288–1330.

13. **McRae A.C., Wei G., Champagne A.R.** Graphene quantum strain transistors // Physical Review Applied. 2019. Vol. 11. No. 5. P. 054019.

14. Ландау Л.Д., Лифшиц Е.М. Теоретическая физика. Т. VII. Теория упругости. М.: Физматлит, 2003. 264 с.

15. Ляпкосова О.С., Лебедев Н.Г. Пьезорезистивный эффект в однослойных углеродных нанотрубках // Физика твердого тела. 2012. Т. 54. № 7. С. 1412–1416.

16. Лебедева О.С., Лебедев Н.Г. Влияние растяжения и сжатия на пьезорезистивность углеродных нанотрубок и графеновых нанолент // Научно-технические ведомости СПбГПУ. Физико-математические науки. 2014. № 1 (189) С. 26–34.

17. Лебедева О.С., Лебедев Н.Г. Пьезорезистивный эффект в примесных однослойных углеродных нанотрубках в приближении «Хаббард-I» // Научно-технические ведомости СПбГПУ. 2014. № 2 (195). С. 149–161.

18. Лебедева О.С., Лебедев Н.Г. Деформационное изменение запрещенной щели примесных углеродных нанотрубок // Химическая физика. 2014. Т. 33. № 10. С. 73–80.

19. Квасников И.А. Термодинамика и статистическая физика. Т. 4. Квантовая статистика. М.: Комкнига, 2005. 352 с.

20. Изюмов Ю.А., Чащин Н.И., Алексеев Д.С. Теория сильно коррелированных систем. Метод производящего функционала. М.: Регулярная и хаотическая динамика, 2006. 384 с.

21. Степанов Н.Ф. Квантовая механика и квантовая химия. М.: Мир. Изд. Московского ун-та, 2001. 519 с.

22. Бир Г.Л., Пикус Г.Е. Симметрия и деформационные эффекты в полупроводниках. М.: Наука, 1972. 584 с.

23. **Lebedeva O.S., Lebedev N.G., Lyapkosova I.A.** Piezoconductivity of chiral carbon nanotubes in the framework of the tight-binding method // Математическая физика и компьютерное моделирование. 2018. Т. 21. № 1. С. 53–63.

24. **Li Y., Wang W., Liano K., Hu Ch., et. al.** Piezoresistive effect in carbon nanotube films // Chinese Science Bulletin. 2003. Vol. 48. No. 2. Pp. 125–127.

25. **Obitayo W., Liu T.** A review: carbon nanotube-based piezoresistive strain sensors // Journal of Sensors. 2012. Vol. 2012. P. ID 652438, 15 p. DOI 10.1155/ 2012/652438.

Статья поступила в редакцию 01.10.2019, принята к публикации 09.12.2019.

СВЕДЕНИЯ ОБ АВТОРАХ

ЛЕБЕДЕВА Ольга Сергеевна – *кандидат физико-математических наук, ассистент Волгоградского государственного университета,* доцент Волгоградского государственного аграрного университета, г. Волгоград, Российская Федерация.
400062, Российская Федерация, г. Волгоград, Университетский пр., 100.
400002, Российская Федерация, г. Волгоград, Университетский пр., 26.
lebedeva_os@volsu.ru

ЛЕБЕДЕВ Николай Геннадьевич – *доктор физико-математических наук, профессор Волгоградского государственного университета,* г. Волгоград, Российская Федерация.
400062, Российская Федерация, г. Волгоград, Университетский пр., 100.
nikolay.lebedev@volsu.ru

ЛЯПКОСОВА Ирина Александровна – *кандидат сельскохозяйственных наук, доцент Волгоградского государственного аграрного университета,* г. Волгоград, Российская Федерация.
400002, г. Волгоград, Университетский пр., 26.
lyapkosova_irina@mail.ru